Journal of Biomedical Optics

SPIEDigitalLibrary.org/jbo

Second-harmonic generation scattering directionality predicts tumor cell motility in collagen gels

Kathleen A. Burke
Ryan P. Dawes
Mehar K. Cheema
Amy Van Hove
Danielle S. W. Benoit
Seth W. Perry
Edward Brown

SPIE

Second-harmonic generation scattering directionality predicts tumor cell motility in collagen gels

Kathleen A. Burke,[a] Ryan P. Dawes,[b] Mehar K. Cheema,[c] Amy Van Hove,[a] Danielle S. W. Benoit,[a,d,e,f] Seth W. Perry,[a] and Edward Brown[a,b,*]

[a]University of Rochester, Department of Biomedical Engineering, 207 Robert B. Goergen Hall, P.O. Box 270168, Rochester, New York 14627, United States
[b]University of Rochester, Department of Neurobiology and Anatomy, 601 Elmwood Avenue, Rochester, New York 14642, United States
[c]State University of New York at Stony Brook, Department of Biomedical Engineering, Stony Brook, New York 11790, United States
[d]University of Rochester, Department of Biomedical Genetics, 601 Elmwood Avenue, Rochester, New York 14642, United States
[e]University of Rochester, Department of Chemical Engineering, 206 Gavett Hall, Rochester, New York 14627, United States
[f]University of Rochester Medical Center, Center for Musculoskeletal Research, 601 Elmwood Avenue, Rochester, New York 14642, United States

Abstract. Second-harmonic generation (SHG) allows for the analysis of tumor collagen structural changes throughout metastatic progression. SHG directionality, measured through the ratio of the forward-propagating to backward-propagating signal (F/B ratio), is affected by collagen fibril diameter, spacing, and disorder of fibril packing within a fiber. As tumors progress, these parameters evolve, producing concurrent changes in F/B. It has been recently shown that the F/B of highly metastatic invasive ductal carcinoma (IDC) breast tumors is significantly different from less metastatic tumors. This suggests a possible relationship between the microstructure of collagen, as measured by the F/B, and the ability of tumor cells to locomote through that collagen. Utilizing *in vitro* collagen gels of different F/B ratios, we explored the relationship between collagen microstructure and motility of tumor cells in a "clean" environment, free of the myriad cells, and signals found in *in vivo*. We found a significant relationship between F/B and the total distance traveled by the tumor cell, as well as both the average and maximum velocities of the cells. Consequently, one possible mechanism underlying the observed relationship between tumor F/B and metastatic output in IDC patient samples is a direct influence of collagen structure on tumor cell motility. [DOI: 10.1117/1.JBO.20.5.051024]

Keywords: second-harmonic generation; multiphoton microscopy; F/B ratio; collagen; metastasis.

Paper 140642SSPR received Oct. 2, 2014; accepted for publication Dec. 9, 2014; published online Jan. 27, 2015.

1 Introduction

Breast cancer is the most frequently diagnosed form of invasive carcinoma and the second leading cause of cancer-induced mortality in the female population.[1] 90% of cancer mortalities are the result of metastasis of the tumor to a secondary location.[2] The tumor stroma, consisting of nontumor cells and the extracellular matrix (ECM), has been known to play a vital role in metastatic efficiency.[3] Collagen, a key component of the ECM, produces an intrinsic optical signal caused by the scattering phenomenon second-harmonic generation (SHG), which allows us to monitor changes in the tumor ECM throughout tumor progression. SHG occurs when two incoming photons scatter off of a noncentrosymmetric structure to produce one emission photon at twice the energy and half the wavelength of the individual incoming photons. SHG emission is coherent, therefore, the directionality of the signal, often quantified through the ratio of the forward-propagating to backward-propagating signal (the F/B ratio), is affected by the properties of a collagen fiber such as fibril diameter, spacing, and order versus disorder in fibril packing within a fiber.[4–6] Collectively, we will herein describe these properties as the collagen fiber "microstructure."[7] Multiphoton imaging of fluorescence and SHG signals has shown that tumor cells move more efficiently along SHG producing fibers than those moving independently of collagen fibers.[8,9] SHG imaging has previously been used to show that in human invasive ductal carcinoma (IDC) breast cancer there is a relationship between tumor collagen microstructure (as indicated by F/B) and the ability of the tumor to metastasize to the lymph nodes.[10] Specifically, primary IDC tumors with a higher F/B ratio significantly produce more metastases in the tumors' draining lymph nodes upon clinical presentation.

The observed relationship between F/B ratio and local metastasis in IDC is interesting for several reasons. New methods to predict metastatic ability of tumors are highly desirable to reduce the problem of "overtreatment" whereby patients receive adjuvant chemotherapy after removal of the primary tumor even though they were not, in fact, destined to get a distant metastasis.[11] Furthermore, exploration of novel pathways governing the metastatic process may reveal new targets for therapeutics to inhibit metastasis. However, the underlying mechanism of the observed relationship between the F/B and IDC metastatic output is currently unclear. This relationship may be entirely due to an ability of collagen microstructure (which determines F/B) to alter tumor cell motility. Alternatively, it may be entirely due to the influence of an upstream actor within the tumor which influences collagen microstructure and tumor cell motility separately. Or it might be a combination of these mechanisms. The goal of this study is to understand the relationship between F/B and tumor cell motility in a relatively "clean" *in vitro* collagen gel system, in which confounding upstream actors are not present.

*Address all correspondence to: Edward Brown, E-mail: Edward_Brown@URMC.Rochester.edu

Collagen gels create *in vitro* environments to study tumor cell motility where, unlike the *in vivo* situation, the presence of extrinsic signals can be closely controlled. In addition to the simplified environmental cues, the alteration of known factors of fibrillogenesis allows for the controlled manipulation of collagen fiber microstructure,[12–14] allowing one to manipulate F/B and hence to explore the relationship between F/B ratio and tumor cell motility. In this work, we change the F/B ratio of collagen gels by three different methods: via alterations in pH, ionic strength [KCl], and collagen I/collagen III ratio. Changing fibrillogenesis using any one of these methods significantly and reproducibly alters the F/B ratio of collagen fibers, allowing us to study how the motility of cells responds to differences in microstructure. Altering F/B using multiple methods helps us to ensure that any consistently observed changes in motility are in response to changes in physical properties of the gel, such as its microstructure, and not due to an alteration of cellular function through an unanticipated direct signaling effect of the fibrillogenesis method (e.g., an alteration in cellular myosin expression in response to changes in the gel's collagen III component). Collagen gel-based techniques have been used in the field of SHG to show that tumor cells more readily travel along aligned collagen fibers,[15] but little has been discovered so far about the relation of fiber microstructure (as indicated by F/B ratio) to tumor mobility. This research will exploit the "clean" environment of collagen gels to provide important insight into the possible mechanisms underlying the relationship between F/B ratio and lymph node metastasis in IDC patients, with the twin goals of improving anti-metastatic treatment and reducing overtreatment.

2 Methods

2.1 *Multiphoton Image Setup and Acquisition*

The following microscopy apparatus was used for the assessment of SHG F/B:

Multiphoton laser scanning microscopy (MPLSM) was conducted using a Ti:Sapphire excitation laser controlled through a BX61WI upright microscope (Olympus, Shinjuku, Tokyo), with beam scanning and image acquisition controlled by an Olympus Fluoview FV300 scanning system. For all imaging, the excitation light was circularly polarized with 100 fs pulses at 80 MHz, where circular polarization at the sample was achieved by passing the excitation light through a Berek compensator (Model 5540, New Focus, Irvine, CA) before entering the scan box. The light was focused through an Olympus UMPLFL20XW water immersion lens (20×, 0.95 N.A.), which was also used to collect the backward propagating SHG and fluorescent signal. Backscattered signals were separated from the excitation beam using a 670 nm short-pass dichroic mirror. The backscattered collagen SHG signal was generated with an excitation wavelength of 810 nm, and the emission was filtered by a 405 nm band-pass filter (HQ405/30m-2P, Chroma, Rockingham, VT). The backward-scattered fluorescence signal, used to image tdTomato-labelled tumor cells, was excited using 740 nm light and the emission signal was filtered using a 580 nm band-pass (HQ580/180m-2P, Chroma) and a 700 nm short-pass filter (E700SP-2P, Chroma). Only SHG was captured in the forward-scattered direction, using an Olympus 0.9 N.A. optical condenser, reflected by a 565 nm long-pass dichroic mirror (565 DCSX, Chroma), and filtered by a 405 nm band-pass filter (HQ405/30m-2P, Chroma). All signals were captured by Hamamatsu HC125-02 photomultiplier tubes.

2.2 *In Vivo Model of Collagen Microstructural Changes*

In order to study the relationship between collagen gel F/B ratio and tumor cell motility, we first identified a tumor cell line that recapitulated in vivo the relationship between F/B and metastatic output observed in patients:

Step 1: Mouse preparation. 40 female BALB/cByJ mice (Jackson Laboratories, Bar Harbor, ME) were anesthetized using ketamine/xylazine (90/9 mg/kg body weight). A cohort of 30 mice received an injection of 5×10^5 tdTomato-labelled 4T1 mouse mammary carcinoma cells in the right inguinal mammary fat pad; the remaining mice were injected with saline. Step 2: Tissue collection. Following 14 days of tumor development and metastasis, the animals were sacrificed using intraperitoneal injection of sodium pentobarbital and subsequent cervical dislocation. Tumors and the draining inguinal lymph node were dissected free of the surrounding tissue and immediately snap-frozen in dry ice. These experiments were performed in accordance with University Committee for Animal Resources regulations. Both tissues were sectioned into 20-μm slices using a cryostat (Reichert-Jung, Depew, NY), mounted onto positively charged slides (VWR) and stored at −20°C until imaged. Step 3: Imaging of tumor sections. Before the start of each imaging session, a standard fluorescein isothiocyanate (FITC) sample was imaged as a calibration sample using 810 nm excitation and 535 nm emission filters (HQ535/40m-2P, Chroma) for both detection systems. Free FITC emits isotropically, but the measured F/B ratio was different from 1.0 each day due to slight variations in the system alignment. Therefore, a calibration factor was determined from the observed F/B ratio of FITC, which was applied to all SHG F/B ratios for that day. In each tumor section, one region was imaged from the center of the tumor, and then four additional regions were imaged by moving the field of view (FOV) in one of four directions from the center (i.e., up, down, left, and right) until the closest visible tumor edge was ~300 μm distant. At each imaged region, both the forward and backward-scattered SHG were acquired in a series of 11 image pairs spaced 3 μm apart to create a 30-μm thick z-stack.

Step 4: Image Analysis: All image analyses was performed with ImageJ software.[16] A maximum intensity projection of each of the two stacks (F and B) reduced the image stacks to a single image pair for each region. On thin (20 μm) tissue sections, these 11 image stacks serve as an autofocus for the thin collagen layer. Each image was background subtracted using the average background value for the corresponding PMT determined by generating an F and B image pair with the laser shutter closed. Next, two masks of both the forward and backward-scattered SHG signals were created in which collagen pixels were set to 1 and background pixels were set to 0 by applying a threshold to each of the two images. The same threshold was applied to all images. This single threshold was chosen by a blinded observer to highlight collagen and to reject background by first surveying a random sampling of images. An example forward-scattered SHG image and the corresponding threshold are shown in Fig. 1(a). After trying different thresholds ranging over ±10 a.u., we found that the F/B ratio of the sample does not significantly differ as a result of different thresholds [Fig. 1(b), ANOVA $p = 0.31$]. The two masks were multiplied together to create one mask that represents pixels with SHG emission above

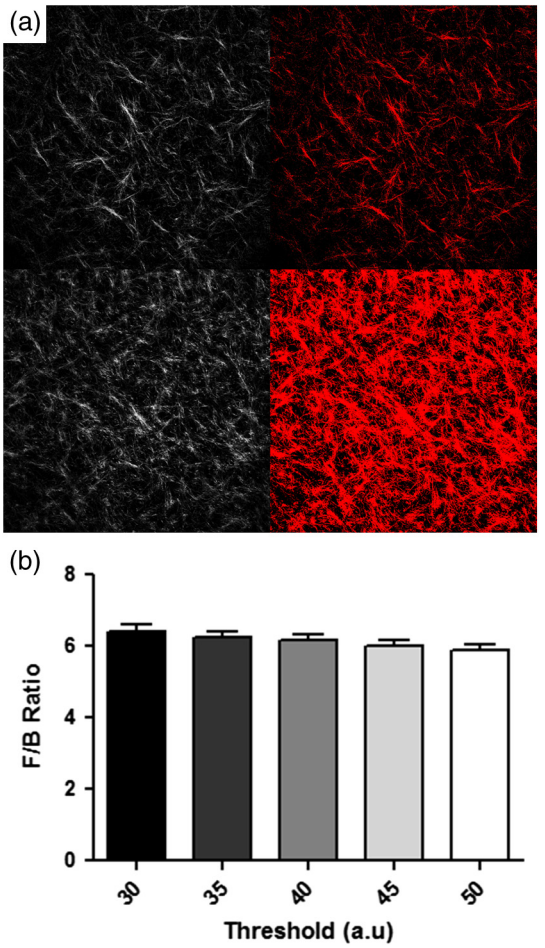

Fig. 1 A threshold is applied to second-harmonic generation (SHG) images in order to highlight the collagen regions. (a) Example backward-scattered (top) and forward-scattered (bottom) SHG image and corresponding thresholded images. (b) Comparison of F/B ratios at different chosen thresholds demonstrates that a 20 a.u. range causes no significant differences in F/B ratio (ANOVA, $p = 0.31$).

the threshold in both the forward and backward directions for that imaged region. A single F/B ratio image for that region was calculated from the F and B image pair. This F/B image was multiplied by the mask in order to set the value of all nonfiber pixels equal to zero, thereby excluding background (i.e., nonfiber) pixels from consideration. The average pixel value of fiber (i.e., nonbackground) pixels for that region was then calculated for each masked F/B ratio image. The five values of F/B for each tumor section were then averaged to determine the average F/B for that section. Note that, as in previous studies,[10] tissue samples were mounted on full thickness glass slides under coverslips, not between two coverslips. While this does not affect the comparisons between identically mounted samples as performed here, the measured F/B of these tissue sections is an underestimate of the true F/B ratio due to the presence of optical aberrations produced by the underlying glass slide.

Step 5: Quantify metastases. To quantify metastasis to the corresponding inguinal lymph nodes, clusters of tdTomato fluorescent cells were counted by a blinded observer on the MPLSM from one section taken from 400 μm within each lymph node. Step 6: Analysis and statistics. All tumors were divided into three groups based on the number of associated metastasis, the "Low" metastasis group had less than four metastases and the "High" group had greater than six metastases. The F/B ratios of the primary tumors were compared between the three groups. Statistical differences were tested using a one-way ANOVA, followed by a Newman–Keuls comparison of all groups. A p-value of $p < 0.05$ was significantly considered.

2.3 *tdTomato Transfected 4T1 Cell Culture*

Once the 4T1 cell line was chosen, it was cultured and eventually seeded on collagen gels:

The tdTomato transfected 4T1 mouse mammary adenocarcinoma cell line (Caliper Life Sciences, Hopkinton, MA) was frozen after three initial passages. After being thawed, each aliquot was used for less than 3 months then replaced from frozen stock. Cells were maintained in RPMI (Gibco, Invitrogen Inc., Carlsbad, CA) containing penicillin/streptomycin and 10% fetal calf serum. All cells were added to the surface of the gels in this media.

2.4 *Preparation of Control Collagen Gels*

Step 1: Dish Preparation. Mattek petri dishes (Ashland, MA) with 14-mm diameter coverslip-bottomed wells were coated with 1% BSA and incubated for 30 min at 37°C and 5% CO_2. Within a sterile hood, the BSA solution was removed and the petri dishes were allowed to dry while preparing the collagen gel solution. Step 2: Making the gel. Gels were made of human type I collagen solution at a concentration of 3 mg/mL, obtained from advanced biomatrix (San Diego, CA). With temperatures maintained at 4°C to minimize collagen polymerization, 810 μl of collagen solution was combined with 108 μl of RPMI media and 50 μl of distilled H_2O. Solutions were gently pipetted to avoid bubble formation in the solution. The pH of the total gel solution was increased between 7.5 and 7.7, using 2.5 M NaOH. 100 μl of solution was aliquoted into each of a maximum of six petri dishes. Step 3: Incubation and imaging. The gels were incubated for 2 h at 37°C. After this period, the gels were covered in phosphate-buffered saline (PBS) in order to avoid dehydration and a subsequent decrease in overall gel volume. Before imaging the PBS was removed from the top of the gel, media containing the appropriate number of cells was added, the gel was cover slipped, and then imaging proceeded immediately.

2.5 *Determining the Effect of Cell Seeding on F/B*

In preliminary experiments, we applied large numbers of cells to the gels and incubated them for 3 days to explore the effects that the cells themselves can have on gel F/B:

Step 1: Cell/Gel preparation. To analyze the effect of cells on the local F/B in a gel, two sets of gels were created: gels with 4T1 cells added to the surface, and identically prepared gels with PBS added to the surface. To seed a gel, 30,000 cells/mL were added to the top of gels in 200 μL of RPMI media and incubated for 3 days, with additional media provided as necessary to prevent drying. Gels without cells were covered in 200 μL of PBS and incubated for 3 days, with addition of PBS if needed to prevent drying. Step 2: Imaging. After removal of gels from the incubator, excess media or PBS was carefully discarded, and the gels were immediately cover slipped and imaged. To quantify the effect of the presence of cells on the local F/B ratio, F/B was determined at one location per gel, chosen to have a high tumor cell density if the gel contained cells, and chosen from the

center of the gel if the gel did not have cells. The images were taken as 660-μm FOV stacks of 11 images spaced 3 μm apart, in order to capture the region of fibers affected by the collagen reorganization. Step 3: Image analysis. These images were maximum intensity projected to produce a single F and B image pair, and then the F/B ratio for the imaged region was determined as described above. Step 4: Comparison: The average F/B ratios of these images were compared between the two gel conditions. Statistical difference was detected using a two-tailed Student's t-test, p-value <0.05.

2.6 *Determining the F/B Ratio of a Collagen Gel*

Next, lower concentrations of cells were applied to gels, and imaged within 3 h to minimize gel remodeling by the cells. Polymerization conditions of the gels were manipulated to vary F/B ratio, and F/B ratio of the gels was determined and evaluated as a function of imaging depth. Finally, the motility of cells within gels of varying F/B ratio was assessed:

Step 1: Calibration. Calibration using a standard FITC sample, and determination of background, were performed as described above. Step 2: Imaging through the gel. For F/B ratio analysis of gels, two stacks of simultaneously collected forward and backward images were taken at the geometric center of each gel, consisting of image pairs taken at 10 μm steps through the depth of the gel. Images were 660 μm across. Step 3: Image analysis. The F/B of each imaged depth was determined as described above. Step 4: Analysis as a function of depth. In order to determine how the measured F/B ratio varied as a function of imaging depth, the F/B ratio was plotted as a function of depth within the gel, in 10% increments by depth. This provides 10 values of F/B ratio for each gel, while allowing for slight differences in the overall depth of the gels (ranging from 450 to 550 μm). A linear fit was applied to each plot to ensure that the slopes of the lines were not significantly different than zero, therefore, ensuring that the measured F/B was not affected by depth into the gel. Step 5: Producing one F/B value. A single value of the average F/B to represent the entire gel was then calculated by taking the average of the F/B ratios taken at each of the 10% depth increments. This value was used in all subsequent comparisons of different gels. All gel comparisons are conducted using a one-way ANOVA, followed by a Newman–Keuls comparison to determine the statistical significance between groups, where $p < 0.05$ was considered statistically significant. Statistical analysis was performed using Prism 5 software (GraphPad, La Jolla, CA).

2.7 *F/B Ratio Manipulation*

The F/B ratio of the gels was altered by manipulating one of three factors within the gel protocol during the previous "Step 2: Making the Gel". The pH was altered by using increasing amounts of NaOH in the final gel solution to bring the total pH to 8.5 to 8.7 or 9.5 to 9.7, measured with a Mettler Toledo Micro Pro pH meter (Columbus, OH). The ionic strength was changed by incorporating potassium chloride (KCl) into the 50 μl dH_2O added to the collagen gel solution at either 100 mM or 200 mM concentrations. The type of collagen forming the matrix was changed by adding increasing amounts of collagen type III by weight, varying from control gels made of 100% collagen type I to experimental conditions of 90% type 1: 10% type III, or 80% type I: 20% type III.

2.8 *Analysis of Tumor Cell Motility*

Step 1: Make gel and add cells. Control gels and F/B ratio manipulated gels were made as previously stated. To dilute out any remaining differences in pH, KCl, or collagen I/collagen III from the polymerization mixture, gels were incubated in 5 mL of PBS for at least 30 min or until each gel was ready to be imaged (maximum of 12 h). Further preparation and imaging was performed one gel at a time. Immediately before imaging, the incubating PBS was removed and 1×10^4 tumor cells resuspended in RPMI media were added to the surface of a single collagen gel in a 200 μL droplet. After allowing the cells to settle onto the gel, the excess media were removed in order to minimize motion during the imaging period. Step 2: Image cells. Live cell images were taken on a Nikon Eclipse Ti, using a Nikon MRH20101 air lens (10x, 0.3 N.A.). Cells were incubated on the microscope stage throughout imaging using a live cell microscope incubator (Pathology Devices, Westminster, MD), at 37°C, 5% CO_2, and 85% relative humidity. One brightfield image was taken every 2 min for 3 h, and saved as a tiff file.

Step 3: Image Analysis. Using the ImageJ[16] "Template Matching" plugin, stacks were aligned through each time point based upon the SHG channel to minimize slight motion artifacts. For each gel, 10 cells (or the maximum number of cells visible) were tracked using the "Manual Tracking" plugin, which tabulates the XY location of each cell at each time point. From these values, the total distance traveled (sum of the distances traveled between each time point), the average velocity (the average of the distance traveled between each time point, divided by the time interval) and the maximum velocity each cell reached over the time course (the largest distance traveled between any two consecutive time points, divided by the time interval) was calculated for each cell and values were averaged across all cells to represent the values of that gel. Note that this is a two-dimensional analysis of tumor cell motility because over the timescales imaged the tumor cells to not penetrate significantly into the gel and their xy motility is significantly greater than their z motility. Allowing the cells sufficient time to significantly penetrate into the gel increases the chances that the cells will alter the F/B of the gel, as discussed above. Step 4: Statistical analysis. Significant differences between the various conditions were determined by comparing the average for each gel using a one-way ANOVA, followed by Newman–Keuls post-hoc comparison of all groups, where $p < 0.05$ was considered statistically significant. Additionally, distance and velocity changes were graphed as a function of the average F/B ratio of the gels and the relationship between the two factors was tested using a Pearson's correlation analysis.

3 Results

3.1 *Animal Model*

It has previously been shown that the average F/B ratio of the primary tumor of patients with IDC varies with the extent of lymph node involvement (i.e., the "N stage") upon clinical presentation.[10] The primary motivation of this study is to understand the relationship between F/B ratio and tumor cell motility in a relatively "clean" *in vitro* collagen cell system, in which confounding upstream effectors are not present. In order to accomplish this, we must first identify a tumor cell line that recapitulates the observed relationship between F/B and lymph node metastasis. This was accomplished by injecting

tdTomato-labeled 4T1 murine mammary adenocarcinoma cells into the mammary fat pad of BALB/c mice. After 2 weeks of growth, tumors were removed along with the draining of the inguinal lymph node [Figure 2(a)], and the F/B ratio of the primary tumor as well as the number of metastases in the lymph node were assessed as described above, to model previous analyses of human samples. As seen in Fig. 2(b), healthy mammary fat pad tissue has a high F/B ratio, which was significantly decreased in a tumor that has a low or medium number of metastasis to the LN. The F/B ratio was not significantly different from healthy mammary fat pad tissue in tumors that had a high number of lymph node metastases. These results exactly match the pattern in human patients with IDC, as shown previously, wherein weakly and moderately metastatic tumors (N0, N1, and N2) exhibited a significantly lower F/B than healthy breast tissue, while highly metastatic tumors (N3) did not.[10]. This suggests that the 4T1 murine mammary adenocarcinoma is a useful model for understanding the relationship between SHG F/B and metastatic output.

3.2 *Creation of Consistent and Optically Thin Collagen Gels*

To evaluate the effect of gel F/B on tumor cell motility, we must next verify that we can produce optically thin gels with consistent F/B ratios. Figure 3(a) shows that the average F/B ratios of control gels were consistent between three different sessions of synthesis and imaging on three different days, demonstrating that the gel formation protocol produces collagen fibers of consistent microstructure. Figure 3(b) shows the average F/B ratio of standard control gels as a function of percent depth into the gel, with the total depths ranging from 450 to 550 μm. These lines were characterized by a slope of zero within the 95% confidence interval, signifying that the measured F/B ratio was not significantly affected by depth, and demonstrating that this method creates optically thin gels, in which the SHG signal was not significantly affected by the thickness of the gel.

3.3 *Manipulation of the Average F/B ratio*

Gels of significantly different F/B ratios were created by changing properties of the collagen gel during fibrillogenesis, including the ionic strength (concentration of KCl), the pH, and the collagen composition (ratio of type I: type III). Figure 4 shows the significant changes in the average F/B ratio of gels resulting from each of the different manipulations, with a significant decrease in F/B ratio as a function of increasing collagen type III and a significant increase in F/B ratio as a function of increasing pH during fibrillogenesis. The relationship between F/B and ionic strength during fibrillogenesis was biphasic, with a peak F/B at 100 mM KCl. The F/B ratio as a function of depth into the gel was a straight line with a slope of 0 within the 95% confidence interval for all gels in all of these conditions (data not shown). Using three methods of changing the F/B ratio allowed us to test how these changes in the collagen microstructure affected the ability of the tumor cells to move along the fibers, while minimizing the chance that this was due to a direct effect of the fibrillogenesis manipulation itself on cell motility, rather than via physical properties of the resulting fibers.

3.4 *Cell Manipulation of Collagen Organization*

The overall motivation for this project was to determine the effects of collagen fiber F/B ratio on the motility rates of tumor cells. However, it has previously been shown that adding tumor cells to collagen gels induces reorganization of the overall collagen fiber morphology.[9] This suggests that tumor cells may also alter the F/B ratio of collagen gels. We found that by adding a large number of cells (3×10^5 cells/mL of media) and allowing a significant amount of time (3 days), the tumor cells were able to induce a significant increase in the F/B ratio of fibers immediately surrounding cell clusters. Figure 5(a) confirms that in regions of high cellular density, the tumor cells alter the local fiber morphology, with fibers in between and surrounding the two clusters of cells becoming straightened and protruding perpendicularly. The regions adjacent to cellular clusters were also characterized by a higher F/B ratio [Figure 5(b)]. This was significant for the design of subsequent

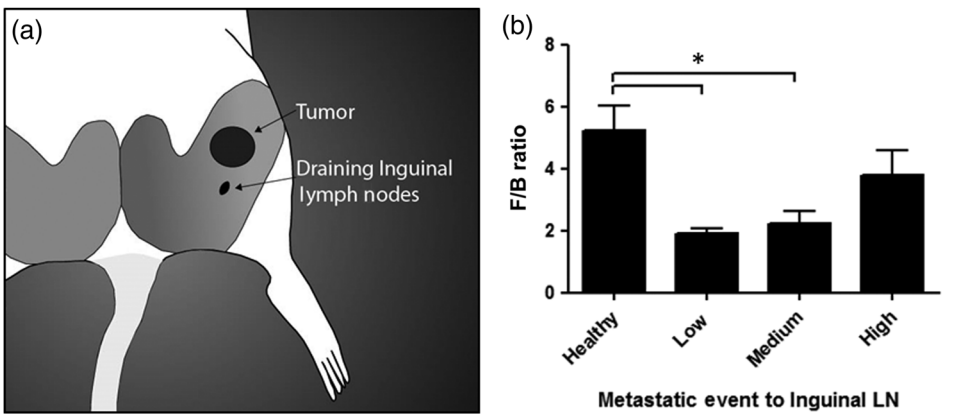

Fig. 2 The relationship between metastasis to LN and SHG F/B in the 4T1 murine mammary adenocarcinoma model matches human data. (a) Diagram of the mouse torso revealing the location of the mammary fat pad where tumor cells were injected and the draining inguinal lymph node. (b) F/B ratio as a function of tumor metastasis to the lymph nodes. The samples are split into four groups: Healthy mammary fat pad (F/B ratio: 5.22 ± 0.79, $n = 10$), Low (1 to 3 mets, F/B ratio: 1.90 ± 0.17, $n = 9$) Medium (4 to 6 m, F/B ratio: 2.24 ± 0.39, $n = 10$), and High (7 to 12 m, F/B ratio: 3.78 ± 0.80, $n = 11$). * represents difference of $p < 0.05$. Results expressed as mean $\pm$ SEM.

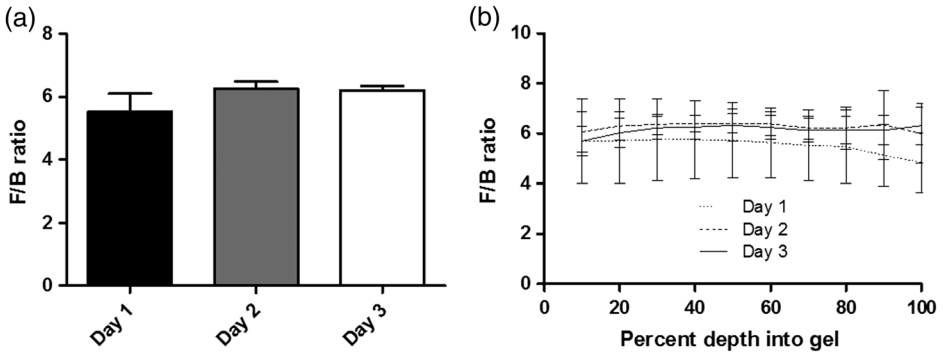

Fig. 3 Control gels revealing consistent collagen gel structure between (a) different synthesis sessions (F/B = 5.52 ± 0.59, 6.27 ± 0.21, and 6.15 ± 0.14) and (b) throughout the depth of the gel. For all plots control $n = 6$. Results expressed as mean ± SEM.

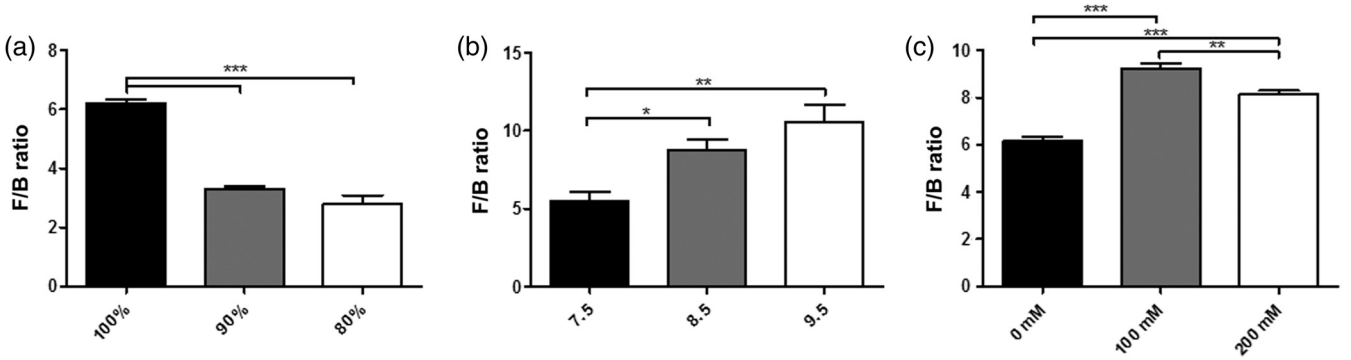

Fig. 4 Methods for significantly changing the F/B ratio. There were significant changes in the average F/B ratio of gels as a function of changes in (a) percent of the collagen in solution that is collagen type I, relative to type III ($n = 6,6,6$), (b) pH of the gel solution ($n = 6,6,6$) and (c) KCl concentration ($n = 6,5,5$). Results expressed as mean ± SEM. * represents difference of $p < 0.05$, ** represents difference of $p < 0.01$, and *** represents difference of $p < 0.001$.

experiments because in order to determine the effect of gel F/B on cell motility, we must prevent the cells themselves from significantly altering the F/B of the gel. For this reason, in the experiments performed subsequently, the cells were added to the surface of the gels in lower concentrations (1000 versus 6,000 cells/gel) and then promptly imaged (3 h versus 3 days), to minimize significant collagen restructuring by the cells.

3.5 *Cell Motility*

Using the methods described above, gels of different average F/B ratio were used to determine how fibers of different microstructure affect the motility of 4T1 mouse mammary tumor cells. Based upon our previous results, we generated gels with four different F/B values using four different methods: gels generated under control conditions had an F/B of 6.20 ± 0.14, gels generated with a collagen I/collagen III ratio of 80% had an F/B of 2.81 ± 0.29, gels generated with 200 mM KCL had an F/B of 8.13 ± 0.16, while gels generated in a pH of 9.5 had an F/B of 10.60 ± 1.08. Note that these alterations are present within the polymerization media during gel fibrillogenesis: during the subsequent seeding and locomotion of tumor cells, which is performed well after the gels are polymerized, the components of the media are the same in all cases. As shown in Figs. 6(a) and 6(b), tumor cells were tracked for 3 h during which the total distance traveled, average velocity, and maximum velocity were measured. There was a significant main effect of the F/B category on total distance traveled (ANOVA $p < 0.05$), and post-hoc analysis revealed that the total distance traveled by cells on gels of the two highest F/B categories was significantly greater than the total distance traveled by cells on gels of the two lowest F/B categories [$p < 0.05$, Fig. 6(c)]. The mechanism by which these tumor cells covered more distance may be related to how efficiently the tumor cells pull themselves along the fiber, which would be revealed through differences in cell velocity. Quantification of the average velocity of cells on gels with different F/B ratios revealed a significant main effect of F/B on average velocity [$p < 0.05$, Fig. 6(d)] while post-hoc analysis revealed that the average velocity of cells on the two highest F/B category gels was significantly higher than the average velocity of cells on the lowest F/B ratio condition. There was also a trend toward increased maximum velocity with increasing F/B ratio [ANOVA $p = 0.06$, Fig. 6(e)]. To quantify the degree to which cell motility and gel F/B ratio are related, a Pearson's correlation analysis and a linear regression were conducted. In these analyses, the F/B groups were formed by collapsing the F/B ratios across treatment conditions to form four distinct F/B ratio groupings, which were compared to the motility data shown in Figs. 5(c) to 5(e). The Pearson analysis revealed a significant positive relationship between F/B ratio and average velocity as well as maximum

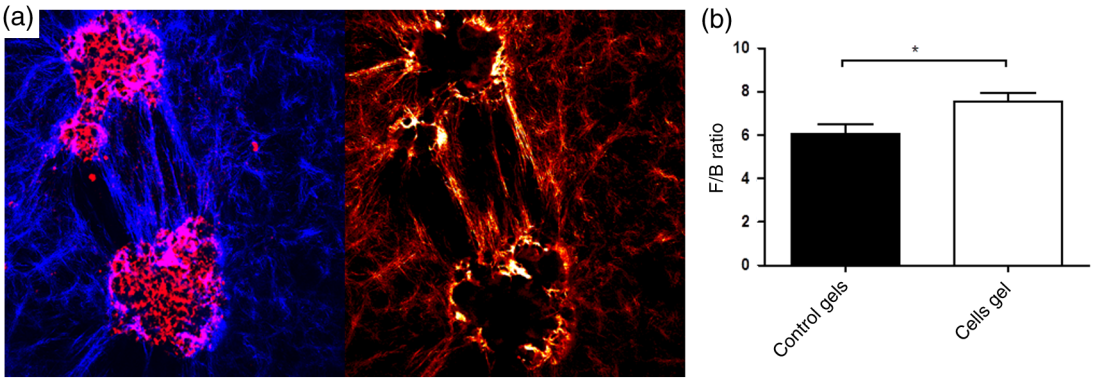

Fig. 5 Collagen restructuring from mouse mammary adenocarcinoma cells. (a) Over 3 days tumor cell (left, red) clusters result in morphological changes in collagen (left, blue) organization in areas surrounding tumor cells, leading to aligned fibers. This also causes changes in the collagen microstructure demonstrated in a heat map of the F/B ratio in the same area (right). (b) Tumor cell clusters can alter local fiber microstructure, depicted by increases in F/B ratio of those fibers (Control $n = 10$, Cell gel $n = 11$). Results expressed as mean ± SEM. *represents $p < 0.05$.

velocity (Figs. 5(g) and 5(h) $p < 0.05$ for both) and a nearly significant relationship between F/B ratio and total distance travelled [Fig. 5(f); $p = 0.06$]. A subsequent regression analysis reveals that these data are closely modeled by a linear fit with a positive slope for the average and maximum velocity ($R^2 = 0.94$ and 0.97, correspondingly). This suggests that these three motility parameters are highly correlated with, and are linearly related to, the F/B ratio.

4 Discussion

In patients with IDC, primary tumors with high values of F/B produce more metastases to the draining lymph nodes upon clinical presentation than tumors with low values of F/B.[10] Gaining a further understanding of the relationship between F/B ratio and metastasis is difficult in the complex *in vivo* environment. On one extreme, the enhanced metastasis effect may be solely due to a direct influence of collagen microstructure (which dictates F/B) on tumor cell motility, while in the other extreme, both F/B and tumor cell motility may be influenced by some unknown upstream players, but not causally related. To further probe the relationship between F/B and metastasis, it is useful to move to the relatively "clean" *in vitro* environment, where tumor cells can interact with collagen gels free of confounding upstream factors.

To probe the *in vitro* relationship between F/B ratio and motility, one must first choose an appropriate cell line. We demonstrate here that the 4T1 murine mammary adenocarcinoma, a common model of triple negative invasive breast cancer, exhibits the same *in vivo* relationship between F/B of the primary tumor and metastasis to draining lymph nodes as seen in human patients, and hence provides an ideal tumor cell line with which to perform these *in vitro* studies. Next, one must find ways to generate collagen gels with different F/B values for the cells to interact with. These results show that we have established methods of creating collagen gels that have reproducible fiber microstructure, and hence a reproducible F/B ratio. These gels are also optically thin; hence, the emitted SHG signal is not significantly affected by subsequent optical scattering within the gel, allowing us to measure the F/B of the gel without concern for the effects of imaging depth. We next determined that varying three characteristics of the gel polymerization protocol: ionic strength, pH, and collagen I/collagen III ratio, allowed us to generate highly reproducible differences in the F/B ratio of the fibers within the gels. By varying these three characteristics, we can produce gels with F/B values ranging over threefold.

Using these cells and gels, we discovered a significant relationship between the collagen gel microstructure (revealed by significant increases in F/B ratio) and the total distance traveled by cells moving through the gels, with a higher F/B resulting in a greater distance traveled. One mechanism by which cells travel this greater distance is by an alteration in the average velocity that the cells move through the gel, as evidenced by the significant relationship between average velocity and F/B ratio. Quantitatively, our results further indicate a linear relationship between total distance traveled and F/B, between average velocity and F/B, and between maximum velocity and F/B. The fact that the changes in F/B ratio were accomplished by three different alterations in the gel polymerization process, and that these alterations were diluted out by a subsequent wash step before cells were applied, help to ensure that the observed differences in motility were due to differences in the physical properties of the resulting gels and not due to a direct effect of polymerization media on subsequent cell motility.

These observations qualitatively match our previous results in human breast tumor samples, where IDC tumors with higher F/B ratio had produced more metastases to the draining lymph nodes than tumors with lower F/B ratio upon clinical presentation:[10] in collagen gels, tumor cells moving through gels with higher F/B travel a greater average distance. Together, these collagen gel experiments suggest that *in vitro* collagen microstructure, as indicated by the F/B ratio, can influence tumor cell motility, and that the observed relationship between metastasis in IDC patients and their primary tumor F/B is due to, at least in part, an effect of tumor collagen microstructure on tumor cell motility. However, the detailed mechanism by which collagen microstructure affects tumor cell motility is not yet clear. Collagen fibril diameter, spacing, and packing disorder within the larger fiber all are known to affect F/B of a given fiber.[4–6] It is possible that changes in these microstructural properties that alter F/B ratio in turn affect the ability of tumor cells to "grip" collagen fibers in such a way as to alter the motility of the cell along the fiber. Alternatively, changes in these microstructural properties that alter F/B may affect the ability of tumor cells to degrade and tunnel through obstructive fibers,

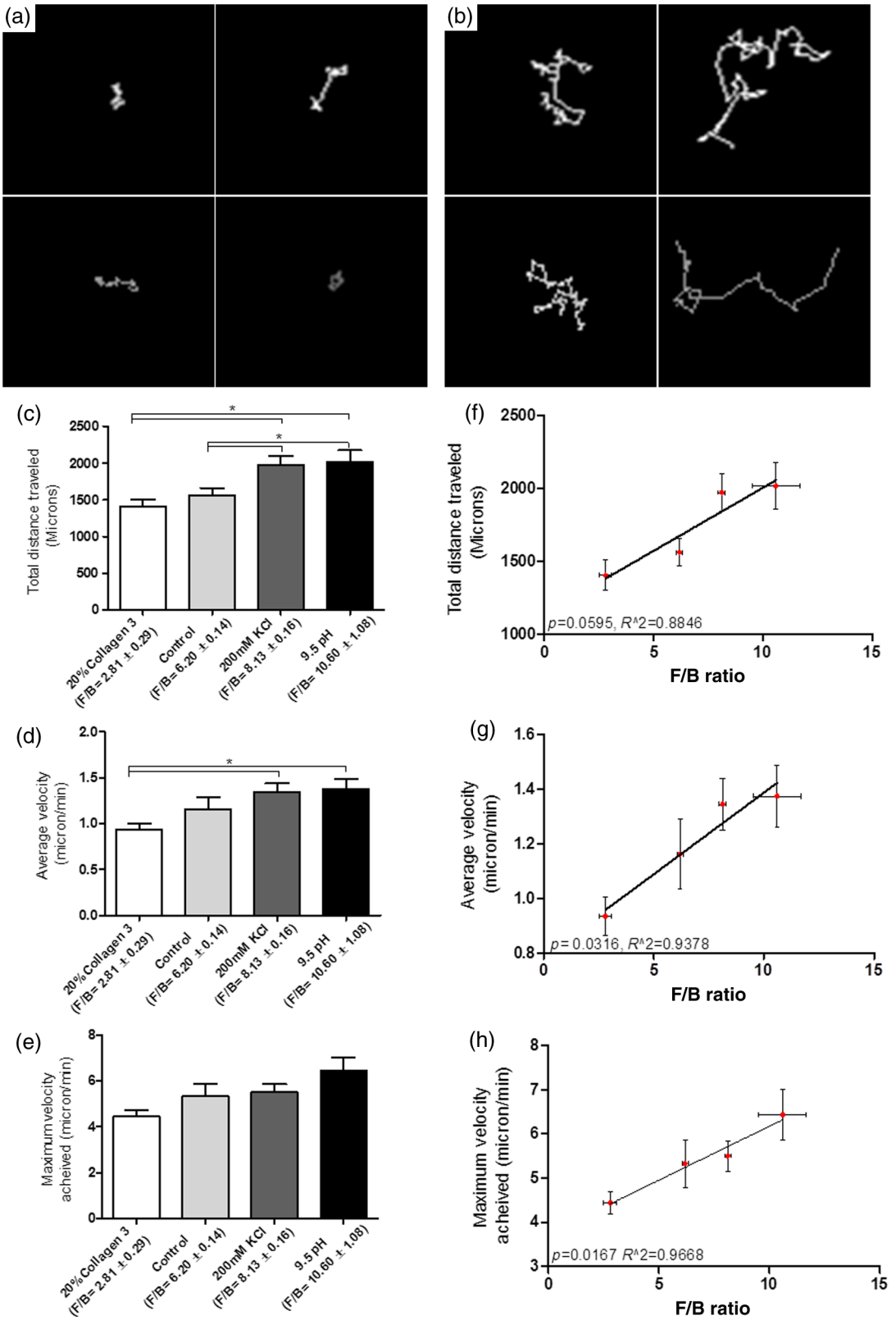

Fig. 6 Effect of synthesis method and F/B ratio on tumor cell motility in collagen gels. Representative tracks of tumor cells over time on low F/B ratio (a) and high F/B ratio (b) gels, qualitatively revealing differences in tumor cell motility. (c) Total distance traveled versus F/B category; ANOVA $p < 0.01$. (d) Average velocity versus F/B category, ANOVA $p < 0.05$. (e) Maximum velocity versus F/B category; ANOVA $p = 0.06$. (f–g) Correlation analyses: (f) Total distance traveled versus F/B value. ($p = 0.06$; $R^2 = 0.88$). (g) Average velocity versus F/B value ($p < 0.05$ and $R^2 = 0.94$). (h) Maximum velocity versus F/B value ($p < 0.05$ and $R^2 = 0.97$). Results expressed as mean ± SEM. For all plots control $n = 6$, for all other conditions $n = 5$. *represents $p < 0.05$ based on Newman–Keuls post-hoc test.

or may be related to the overall extent of obstructions present. Additionally, alterations in these microstructural properties that alter F/B may affect the overall stiffness of the collagen, leading to stiffness-sensitive alterations in tumor cell locomotion.[17] Or a combination of these effects may contribute to the relationship between F/B and motility.

In preliminary studies, we determined that at high seeding densities and over long time periods, the 4T1 cell line used here can alter the F/B of the local collagen matrix. This led us to restrict these experiments to lower seeding densities and significantly shorter time periods in order to minimize this effect, and allowed us to evaluate the effect of gel F/B on tumor cells, not the effect of tumor cells on gel F/B. However, this novel observation that tumor cells locally affect collagen F/B ratio *in vitro* offers additional insight. First, the reorganization of the direction and shape of the fibers correlates with a change in collagen microstructure that can be detected through changes in the F/B ratio. This finding suggests that the processes by which morphology and microstructure are modified by tumor cells are linked. Furthermore, we have previously shown that altering the availability of stromal MMP-13 altered F/B and metastatic output.[18] The fact that tumor cells themselves can affect F/B (as shown here), and that alteration of enzymes present in the stroma can alter F/B (as shown previously), suggests that both tumor and stromal cells play key roles in defining the matrix microstructure that dictates F/B.

5 Summary

In summary, these results suggest that the relationship between F/B and metastatic output observed in patient IDC samples can be explained at least in part by a direct influence of collagen microstructure on tumor cell motility. Further exploration of the underlying mechanisms of this relationship may lead to anti-metastatic drugs that reduce clinical metastasis by altering tumor collagen microstructure. Furthermore, these results also suggest that in the future, quantitative measurements of the state of collagen microstructure, i.e., F/B, may be useful to predict the metastatic capability of a primary tumor, and subsequently the overall survival of individual patients. The development of improved methods of predicting metastatic outcome would help to reduce the problem of overtreatment, where patients are treated with adjuvant chemotherapy who would otherwise not have suffered a metastasis.[11] Finally, these results reveal that the tumor cells themselves directly modify the collagen microstructure, altering the local F/B ratio, in addition to the previously known role that stromal cells play in this remodeling.

Acknowledgments

Funding for this research was provided by the NIH [Director's New Innovator Award: DP2 OD006501 (EB), R01AR064200 (DB)], the Department of Defense [Era of Hope Scholar Research Award: W81XWH-09-1-0405 (EB)], the National Science Foundation [DMR1206219 (DB)], and New York State Stem Cell Science [NYSTEM, N11G-035 (DB)]. Kathleen Burke was supported by National Institutes of Health under Award No. F31CA183351 and Award No. T32AI007285; Ryan P. Dawes was supported by the NIH Training Grant in Neuroscience Award No. 5T32NS007489-13; and Amy Van Hove was supported by a Howard Hughes Medical Institute Med-into-Grad fellowship. Seth W. Perry was supported by NIH Exploratory Developmental Research Grant Award No. R21DA030256.

References

1. American Cancer Society, *Cancer Facts & Figures 2012*, American Cancer Society, Atlanta (2012).
2. E. R. Fisher et al., "The pathology of invasive breast cancer. A syllabus derived from findings of the national surgical adjuvant breast project (protocol no. 4)," *Cancer* **36**(1), 1–85 (1975).
3. R. R. Langley and I. J. Fidler, "The seed and soil hypothesis revisited—The role of tumor-stroma interactions in metastasis to different organs," *Int. J. Cancer* **128**(11), 2527–2535 (2011).
4. X. Han et al., "Second harmonic properties of tumor collagen: determining the structural relationship between reactive stroma and healthy stroma," *Opt. Express* **16**(3), 1846–1859 (2008).
5. R. Lacomb et al., "Phase matching considerations in second harmonic generation from tissues: effects on emission directionality, conversion efficiency and observed morphology," *Opt. Commun.* **281**(7), 1823–1832 (2008).
6. R. M. Williams, W. R. Zipfel, and W. W. Webb, "Interpreting second-harmonic generation images of collagen I fibrils," *Biophys. J.* **88**(2), 1377–1386 (2005).
7. R. M. Burke et al., "Tumor-associated macrophages and stromal TNF-α regulate collagen structure in a breast tumor model as visualized by second harmonic generation," *J. Biomed. Opt.* **18** (8), 086003 (2013).
8. J. Condeelis and J. E. Segall, "Intravital imaging of cell movement in tumours," *Nat. Rev. Cancer* **3**(12), 921–930 (2003).
9. P. P. Provenzano et al., "Collagen reorganization at the tumor-stromal interface facilitates local invasion," *BMC Med.* **4**(1), 38 (2006).
10. K. Burke, P. Tang, and E. Brown, "Second harmonic generation reveals matrix alterations during breast tumor progression," *J. Biomed. Opt.* **18**(3), 31106 (2013).
11. B. Weigelt, J. L. Peterse, and L. J. van't Veer, "Breast cancer metastasis: markers and models," *Nature Reviews. Cancer* **5**(8), 591–602 (2005).
12. V. Ajeti et al., "Structural changes in mixed Col I/Col V collagen gels probed by SHG microscopy: implications for probing stromal alterations in human breast cancer," *Biomed. Opt. Express* **2**(8), 2307–2316 (2011).
13. C. B. Raub et al., "Noninvasive assessment of collagen gel microstructure and mechanics using multiphoton microscopy," *Biophys. J.* **92**(6), 2212–2222 (2007).
14. B. A. Roeder, K. Kokini, and S. L. Voytik-Harbin, "Fibril microstructure affects strain transmission within collagen extracellular matrices," *J. Biomech. Eng.* **131**(3), 031004 (2009).
15. P. P. Provenzano et al., "Contact guidance mediated three-dimensional cell migration is regulated by Rho/ROCK-dependent matrix reorganization," *Biophys. J.* **95**(11), 5374–5384 (2008).
16. C. A. Schneider, W. S. Rasband, and K. W. Eliceiri, "NIH Image to ImageJ: 25 years of image analysis," *Nat. Methods* **9**(7), 671–675 (2012).
17. C.-M. Lo et al., "Cell movement is guided by the rigidity of the substrate," *Biophys. J.* **79**(1), 144–152 (2000).
18. S. W. Perry et al., "Stromal matrix metalloprotease-13 knockout alters Collagen I structure at the tumor-host interface and increases lung metastasis of C57BL/6 syngeneic E0771 mammary tumor cells," *BMC Cancer* **13**(411) (2013).

Biographies of the authors are not available.